nature geoscience

LETTERS

PUBLISHED ONLINE: 12 JANUARY 2014 | DOI: 10.1038/NGEO2047

Emergence of oblique dunes in a landscape-scale experiment

Lü Ping[1,2]*, Clément Narteau[2]*, Zhibao Dong[1], Zhengcai Zhang[1] and Sylvain Courrech du Pont[3]

Aeolian dunes in many arid environments on Earth are shaped by seasonally varying bimodal wind regimes. However, the dynamics of dune evolution under such wind regimes are difficult to investigate at the time and length scales of laboratory experiments[1]. These bedforms, in their natural environments[2–4], may also be influenced by unknown initial conditions and a variety of factors such as sediment availability[5], vegetation[6] and cohesion[7]. Here we report results from a landscape-scale experiment in which we examine the evolution of bedforms under asymmetric bimodal winds. After flattening an experimental dunefield across 16 hectares of the Tengger Desert in Inner Mongolia, we measured winds and topography from March 2008 to October 2011 to reveal the development of regular dune patterns with a constant wavelength and increasing amplitude. On a seasonal timescale, we show that individual dunes propagate in different directions according to the prevailing wind. We find that the orientation of dune crests is controlled by the combination of the normal contributions of the two dominant winds, with respect to their relative strengths and directions, such that crests form an oblique angle of 50° with the resultant sand flux. Our landscape-scale experiment suggests that the alignment of aeolian dunes can be used to determine wind forcing patterns on the Earth and other planetary bodies.

Desert areas exhibit a wide range of regular dune patterns that are the most recognizable landscapes resulting from aeolian activity on Earth and other planetary bodies. Formed by unidirectional winds in zones of high sediment availability, transverse dunes exhibit a periodic alignment of crests perpendicular to the flow[8]. At the other end of the spectrum of complexity, dunefields under multidirectional wind regimes may be covered with star dunes, majestic sand hills with arms radiating in various directions[9]. However, the seasonality of the climatic forcing in the subtropics implies that many arid environments on Earth are submitted to bimodal wind regimes. Under such conditions, it is commonly accepted that dunes tend to align in the direction for which the sum of the normal to crest components of the transport vectors reaches its maximum value[10]. Using this so-called gross bedform-normal transport rule, straight-crested dunes may then be documented and classified considering only the angle between crest orientation and the resultant sand transport direction. In practice, when the deviation is less than 15° from the perpendicular and the parallel alignments, dunes are recognized as transverse and longitudinal dunes, respectively. In all other cases, straight-crested dunes are considered as oblique. Although transverse and longitudinal dunes have been reproduced in subaqueous laboratory experiments[11–13] and numerical simulations[14–16], there are only a few limited observations on the dynamics of oblique dunes in aeolian settings[17–20]. This is partly because these dynamics occur on timescales that are much longer than those of the remote sensing data and partly because there are no complete long-term records of local climatic variables in desert areas.

Moreover, dunes are difficult to reproduce in wind tunnel experiments. The main reason is that the characteristic length scale λ_{max} for the formation of dunes is proportional to the saturation length, the distance needed for the sand flux to adapt to a change in wind strength[21,22]. Accordingly, the λ_{max}-value is of the order of 20 m for aeolian dunes on Earth. This minimum dimension, combined with the difficulty of varying flow orientation, makes laboratory experiments on oblique dunes overly complicated. Hence, there is not yet any experimental data about the formation and the development of oblique aeolian dunes, so that their very existence remains open to intense scientific debate[2].

Here we analyse the outcomes of a landscape-scale experiment to image dune morphodynamics over timescales of years in the Tengger Desert (Fig. 1). This southernmost region of the Gobi Desert has a typical continental monsoon climate with less than 180 mm of annual precipitation. The average temperature ranges between 24.3 °C in July and −6.9 °C in January. In such a cold desert, shifting dunes free of vegetation form a dune network with northeast–southwest primary ridges and north–south secondary ridges[23]. Previously, these two sets of dune crests have been described as transverse to the two dominant winds[24], which are mainly regulated by the dynamics of the Siberian–Mongolian high-pressure cell. During winter, Central Asia experiences a pronounced heat loss leading to the development of a persistent northwesterly wind across western China. In summer, the surface of the Asian continent gains heat and the dominant atmospheric systems are thermal depressions and easterly winds induced by the East Asian monsoon.

The main objective of the landscape-scale experiment is to characterize and quantify the development of bedforms in a natural aeolian environment using controlled initial and boundary conditions. Working at a length scale that is significantly larger than the initial wavelength λ_{max} for the formation of dunes, 16 hectares of the dunefield were flattened on the 20 December 2007 using a bulldozer (Fig. 1a). Then, three experimental areas were designed for comparison between different types of boundary condition (Fig. 1b). At the same site and before flattening, an automatic wind measurement system was installed at the top of a meteorological tower of 10 m height. It records the mean wind speed and direction

[1]Key Laboratory of Desert and Desertification, Cold and Arid Regions Environmental and Engineering Research Institute, Chinese Academy of Sciences, 320 West Donggang Road, Lanzhou 730000, Gansu, China, [2]Institut de Physique du Globe de Paris, Sorbonne Paris Cité, Univ Paris Diderot, UMR 7154 CNRS, 1 rue Jussieu, Paris 75238, Cedex 05, France, [3]Laboratoire Matière et Système Complexes, Sorbonne Paris Cité, Univ Paris Diderot, UMR 7057 CNRS, Bâtiment Condorcet, 10 rue Alice Domon et Léonie Duquet, Paris 75205, Cedex 13, France. *e-mail: lvping@lzb.ac.cn; narteau@ipgp.jussieu.fr

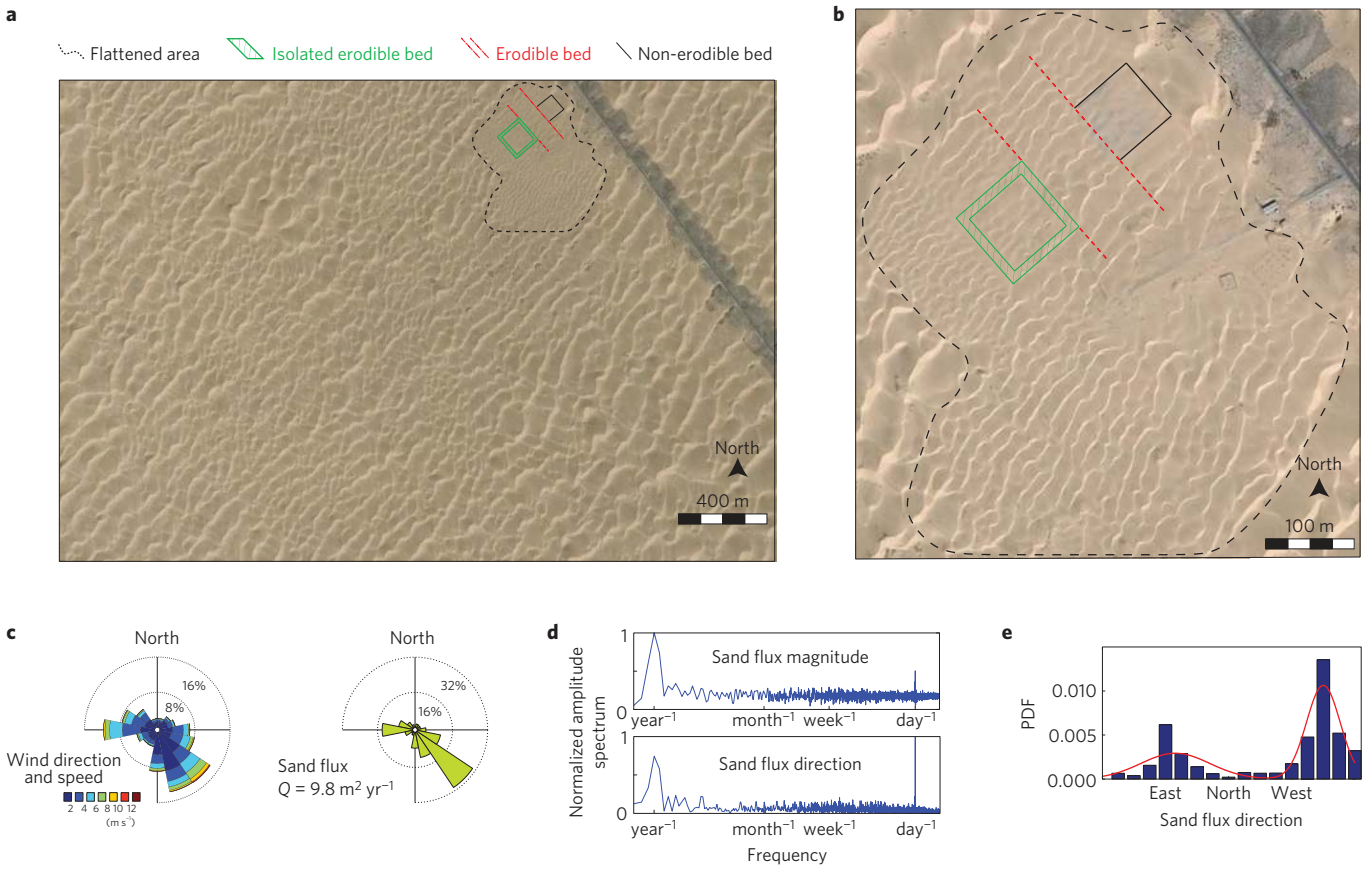

Figure 1 | The landscape-scale experiment site in the Tengger Desert. a,**b**, The flattened area at two different length scales (37° 33′ 43.5″ N,105° 2′ 5.20″ E). The three experimental plots are an open corridor (red), a closed area isolated from external sand flux by a straw chequerboard (green) and a non-erodible bed covered with gravel (black). **c**, Wind and sand flux roses calculated using the wind data of the local meteorological tower from 1 January 2008 to 31 December 2011 (Supplementary Information). **d**, Normalized amplitude spectra of the magnitude and the orientation of sand flux. **e**, The probability density function (PDF) of sand flux orientation and the best fit using a two-component Gaussian mixture model (Methods).

every minute. Figure 1c shows the wind and sand flux roses for four years from the flattening date. As expected, from the long-term meteorological data, there is a clear bimodal wind regime with a primary peak in the southeast direction and a secondary peak in the west direction. Spectral analysis clearly shows annual and daily variations in both speed and orientation (Fig. 1d). Superimposed to the seasonal cycle, the daily period may be explained by a contrast in heat capacity between the desert area and the surrounding lands. Most importantly, Fig. 1e shows that the bimodal wind regime may be described by a divergence angle of 149° and a transport ratio of 2 (equation (1), Methods).

We concentrate here on the evolution of erodible beds and analyse the data collected in the open corridor of 120×80 m^2 and in the closed area of 80×80 m^2. From March 2008 to October 2011, as these winds pile the flat sand bed into dunes, regular topographic measurements of the open corridor show the development of a surface undulation with a constant wavelength of 23 m (Fig. 2a) and an increasing amplitude (Fig. 2b). The emergence of regular patterns with a well-defined wavelength may be associated with the linear regime of the dune instability mechanism[22,25] and the most unstable wavelength λ_{max} for the formation of dunes. Unfortunately, it is impossible to conclude about the exponential growth rate of this instability as the amplitude varies only from 1 to 2 m from the first to the last topographic measurement separated by nearly 42 months. In addition, given that this amplitude has already reached a height of 1 m three months after flattening at the time of the first topographic survey, it is clear that the characterization of the early growth phase requires more frequent measurements, particularly at the beginning of the experiment before the development of slip faces.

Nevertheless, the ongoing experiment covering a period of almost four years in a zone with an estimated sand flux of approximately 10 m^2 yr^{-1} (Fig. 1c) and bedforms of less than 3 m in amplitude (Fig. 2b) provides a unique data set for the analysis of the morphodynamics of individual dunes. Figure 3 shows that, in the open corridor and the closed area, isolated dune features migrate in different directions according to the seasonal wind regime. Not surprisingly, westward displacements during summer 2010 are followed by southeastward displacements during winter. For the last time period during which the two winds are present, dunes move and stretch along an intermediate direction almost perpendicular to the resultant sand transport vector (Fig. 3d). As these dunes are propagating, they grow and align along a specific direction.

To determine the orientation of any topographic features, we look for sand volumes above a reference height and calculate the principal directions of their mass distribution matrix as well as their centre of mass (Supplementary Information). Thus, we can derive quantitative estimates of isolated dune motions (Fig. 3d) and bedform orientation in more than 170 independent circular parcels of the open corridor. Averaging over all these parcels, we find that the global alignment of the observed dune patterns is permanently evolving between the two directions perpendicular to the two dominant winds (Fig. 4a). Eventually, the dune trend converges to an intermediate direction that is more perpendicular

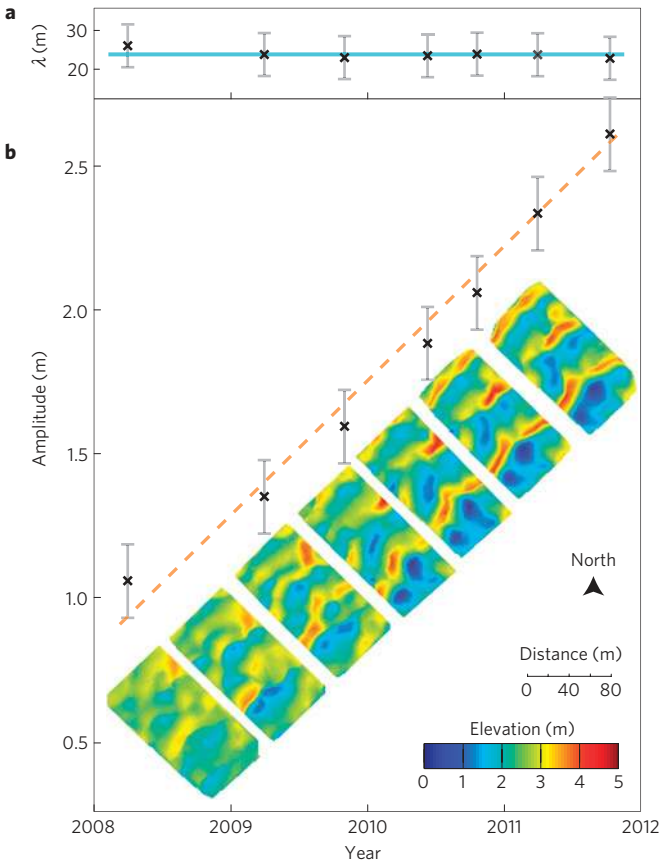

Figure 2 | Development of surface undulations in the open corridor. **a**, Characteristic wavelength of surface undulations with respect to time. The horizontal line corresponds to a constant wavelength of 23 m. **b**, Amplitude of surface undulations with respect to time. The dashed line has a slope of 0.41 m yr^{-1}. Insets show the evolution of topography. Amplitude and wavelength are calculated from the autocorrelation function of the bed profile using 70 transects. The amplitude is twice the square root of two times the standard deviation. The wavelength is the mean position of the first peak. Error bars are the corresponding standard deviations.

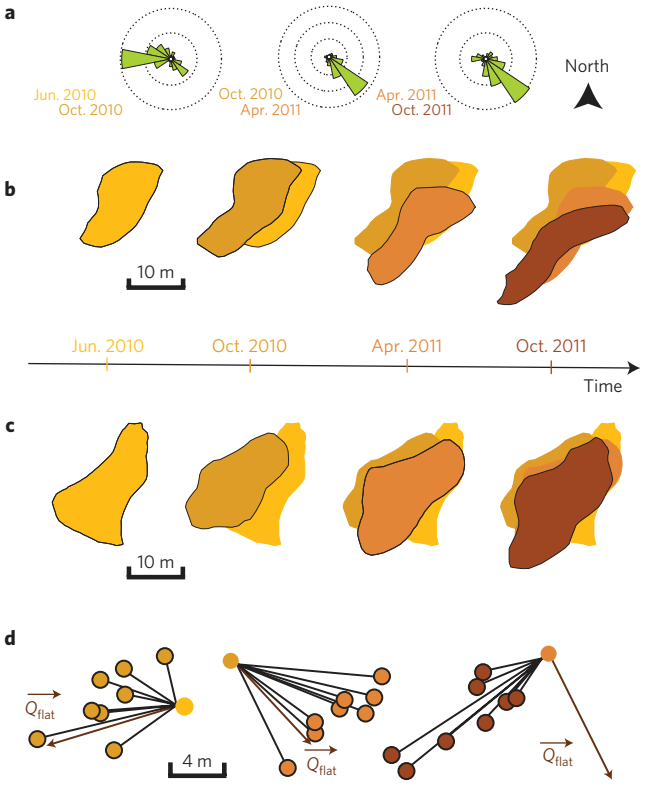

Figure 3 | Morphology and dynamics of individual dunes according to seasonal winds. **a**, Sand flux roses using the local wind data (Supplementary Information). The three consecutive time periods are characterized by easterly (summer 2010), northwesterly (winter 2010–2011) and bimodal (summer 2011) wind regimes. **b**,**c**, Evolution of a dune shape in the open corridor and the closed area. At all times, contours are isolines of equal elevation. **d**, Horizontal displacements of the centre of mass of eight individual dunes. Brown arrows show the resultant sand flux direction. Note the different phases of dune migration with respect to the wind regime.

to the primary wind. This orientation is in good agreement with the prediction of the gross bedform-normal transport rule[10] that can be independently derived from the wind data (Supplementary Information). Overall, there is an angle of 50° between the orientation of the ridges and the resultant sand transport direction (Fig. 4b), so that the bedforms of the open corridor can be defined as oblique dunes. Furthermore, Fig. 4a shows also that changes in orientation estimated from the topographic data are consistent with the variations that can be expected from the wind data alone. These similar behaviours indicate that, when the dune patterns are growing in a zone of high sediment availability, their alignment may be directly related to the climatic forcing using only estimates of the normal to crest components of transport.

This cross-crest component of transport varies according to wind orientation and because of changes in the apparent dune aspect ratio[9,26]. Then, when the winds blow alternately on either side of the dune, a persistent asymmetry in normal transport properties will gradually result in a shift of the entire structure in the direction of the prevailing flux[27]. By definition, oblique dunes are therefore likely to migrate laterally with respect to the orientation of their crests[17,28]. The present field measurements confirm such lateral migration for two asymmetric winds with a divergence angle of more than 90°. In fact, the resultant sand transport direction has an eastward component of transport that is significantly more pronounced than those of individual bedform motions that have been identified in the open area or the closed area (Figs 3 and 4b). This is consistent with the fact that dunes grow in height using normal to crest components of transport. If we extrapolate such a lateral dune migration to larger length scales and timescales, it may explain how the Tengger Desert has been able to extend southward from the sedimentary resources of the Badain Jaran sand sea[29].

The landscape-scale experiment is a new concept in geomorphology that is particularly well suited for validation and quantification purposes[30]. Given the extreme conditions encountered in arid deserts and the timescales associated with the development of bedforms, *in situ* experiments on aeolian sand dunes have to combine logistics facilities with long-term measurements. By successfully meeting these challenges, we obtain here the first experimental evidence for the formation of oblique aeolian dunes. In addition, we verify that, in a zone of high sediment availability, these oblique dunes align in a direction that can be predicted from the cross-crest components of transport. Thus, the observed crest orientation sums the contribution of all winds with respect to their relative strength and orientation. It is notable that this property can then be used to evaluate the variability of wind directionality from the morphology of reversing dunes. We also show that oblique dunes migrate laterally, which has important implications for the dynamics of desert areas. Eventually, as a result of the seasonality in wind forcing, oblique dunes are likely to be widely present on Earth and other planetary bodies, such as Mars and Titan. Thus,

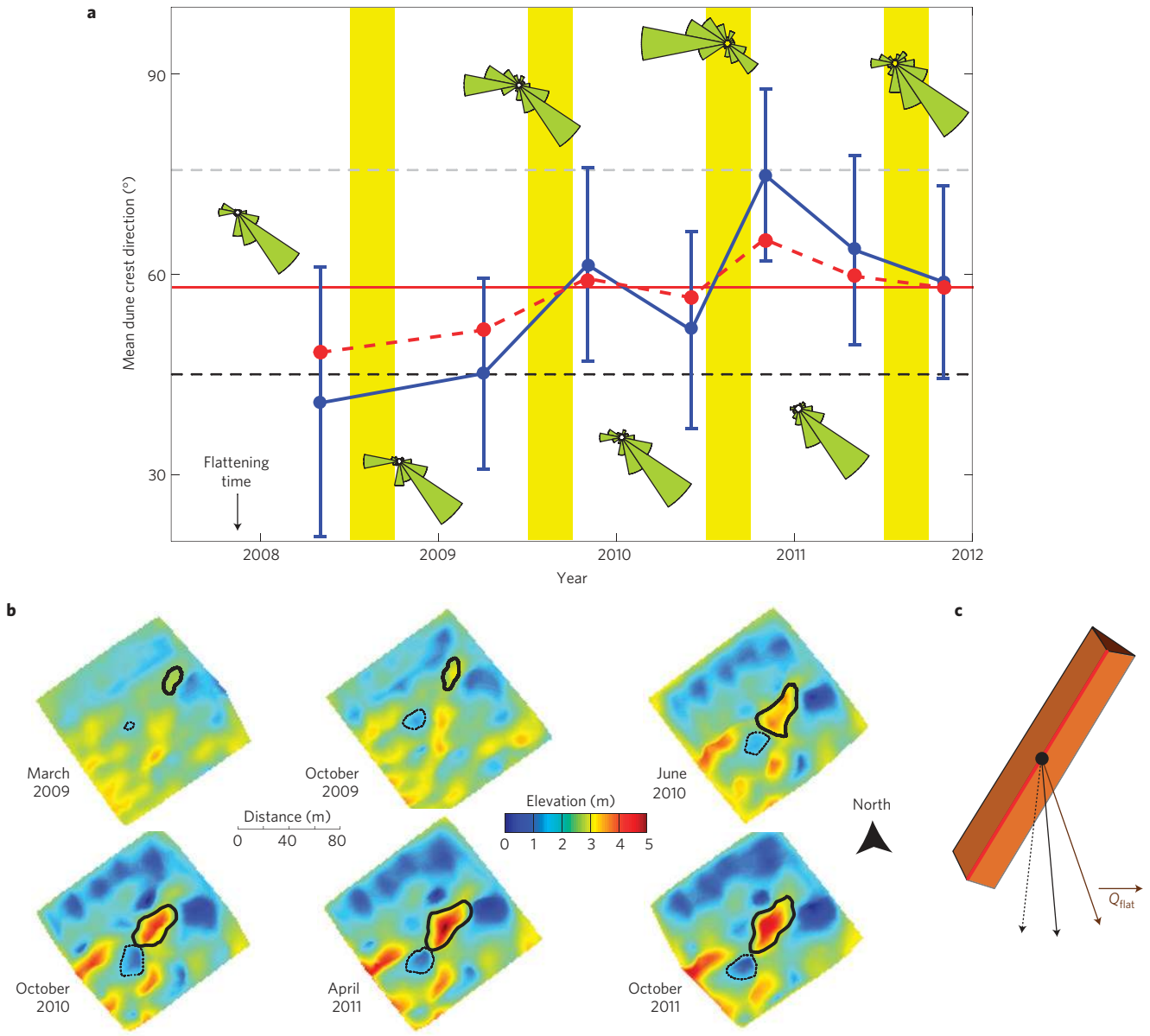

Figure 4 | Oblique bedform alignment and lateral dune migration. a, Observed (blue) and predicted (red) dune orientations in the open corridor using topographic surveys and the gross bedform-normal transport rule with the local wind data from the flattening time. Sand flux roses (green) are derived from wind measurements during the corresponding time intervals. All directions are measured anticlockwise from east. Error bars are standard deviations for circular parcels with radius of 7.5 m (Supplementary Information). Horizontal lines show the last predicted value (red) and the directions perpendicular to the primary (black) and the secondary (light grey) winds. Yellow bands show the summer periods when the secondary wind is likely to prevail. **b**, Evolution of topography in the closed area. Contours highlight the positions of a dune (solid) and a trough (dashed). **c**, Displacement vectors of this dune (solid) and this trough (dotted) show lateral migration between the resultant sand flux direction (brown vector) and the crest alignment (red line).

their identification can lead to new estimates of the overall sediment transport and better constraints on global circulation models.

Methods

The closed area is isolated from external sand flux using a straw chequerboard barrier with a width of 20 m (dashed green area in Fig. 1a,b), a distance that is much larger than the saturation length. This sand barrier consists of a regular lattice of narrow bands of straw (for example, wheat, rice, reed of 40 cm height) overlying the erodible bed. Half of the plant is buried and the other half is exposed to the air, offering a substantial resistance to the flow. Thus, as the wind blows on a straw chequerboard barrier, the bed shear stress is decreasing with distance (that is, deposition) to finally fall below its critical value for sediment entrainment (that is, no transport).

The resolution of the topographic survey is 0.5 m using a Topcon G7200L theodolite. All measurements are relocated according to four reference points for each experiments. Basically, they are located at the corner of the squares limiting the non-erodible bed and the closed area (black and green squares in Fig. 1a,b). The main reference point is a block of concrete at the southern corner of the non-erodible bed (37°33′ 45.9″ N, 105°1′ 55.4″ E).

We use an expectation–maximization algorithm to fit the sediment flux orientation distribution by a Gaussian mixture model. Thus, we replace the fluxes derived from the wind data by a limited number n_Θ of flux vectors characterized by a mean orientation Θ_i and a weight w_i with $i = \{1, \ldots, n_\Theta\}$. Considering only time periods during which the wind velocity is above a critical value for sediment transport (Supplementary Information), we assume that the probability distribution function of sand flux orientation Θ may be described by a sum of normal distributions:

$$\mathcal{P}(\Theta) = \sum_{i=1}^{n_\Theta} \frac{w_i}{\sigma_i\sqrt{2\pi}} \exp\left(-\frac{(\Theta-\Theta_i)^2}{2\sigma_i^2}\right) \quad (1)$$

where σ_i is the standard deviation of wind orientation in the direction Θ_i. The expectation–maximization algorithm is a natural generalization of maximum

likelihood estimation to the incomplete data case. Basically, this is an iterative scheme that includes two different steps. Starting from initial guesses for the parameters w_i, σ_i and Θ_i, the expectation step is to compute a probability distribution over possible completions. In the maximization step, new parameters are determined using the present completions. These steps are repeated until convergence. Figure 1e shows the histogram of sand flux directionality in the landscape-scale experimental site and how it can be fitted with a two-component Gaussian mixture model ($n_\Theta = 2$). All angles are measured anticlockwise from east. For the sand flux produced by the northwesterly wind we have

$$w_1 = 0.64, \quad \Theta_1 = 315^\circ, \quad \sigma_1 = 24^\circ$$

For the sand flux produced by the easterly wind we have

$$w_2 = 0.36, \quad \Theta_2 = 166^\circ, \quad \sigma_2 = 49^\circ$$

Thus, there is a prevailing wind ($w_1 > w_2$) and we can estimate the transport ratio $R = w_1/w_2 \approx 2$ as well as the angle of divergence $\gamma = \Theta_1 - \Theta_2 = 149^\circ$ between the primary and secondary winds. These two variables are enough to predict dune crest orientation using the analytical solution of the gross bedform-normal transport rule[10]. However, this can also be done with more precision using the entire wind data set and the cross-crest components of transport (Supplementary Information).

Received 15 July 2013; accepted 25 November 2013; published online 12 January 2014

References

1. Hersen, P., Douady, S. & Andreotti, B. Relevant length scale of barchan dunes. *Phys. Rev. Lett.* **89,** 264301 (2002).
2. Pye, K. & Tsoar, H. *Aeolian Sand and Sand Dunes* (Unwin Hyman, 1990).
3. Cooke, R., Warren, A. & Goudie, A. *Desert Geomorphology* (UCL Press, 1993).
4. Lancaster, N. *Geomorphology of Desert Dunes* (Routledge, 1995).
5. Wasson, R. & Hyde, R. Factors determining desert dune type. *Nature* **304,** 337–339 (1983).
6. Thomas, D. S. G. & Tsoar, H. in *Vegetation And Erosion* (ed. Thornes, J. B.) 471–489 (Wiley, 1990).
7. Rubin, D. & Hesp, P. A. Multiple origins of linear dunes on Earth and Titan. *Nature Geosci.* **2,** 653–658 (2009).
8. Zhang, D., Narteau, C. & Rozier, O. Morphodynamics of barchan and transverse dunes using a cellular automaton model. *J. Geophys. Res.* **115,** F03041 (2010).
9. Zhang, D., Narteau, C., Rozier, O. & Courrech du Pont, S. Morphology and dynamics of star dunes from numerical modelling. *Nature Geosci.* **5,** 463–467 (2012).
10. Rubin, D. & Hunter, R. Bedform alignment in directionally varying flows. *Science* **237,** 276–278 (1987).
11. Rubin, D. & Ikeda, H. Flume experiments on the alignment of transverse, oblique, and longitudinal dunes in directionally varying flows. *Sedimentology* **37,** 673–684 (1990).
12. Reffet, E., Courrech du Pont, S., Hersen, P. & Douady, S. Formation and stability of transverse and longitudinal sand dunes. *Geology* **38,** 491–494 (2010).
13. Taniguchi, K., Endo, N. & Sekiguchi, H. The effect of periodic changes in wind direction on the deformation and morphology of isolated sand dunes based on flume experiments and field data from the Western Sahara. *Geomorphology* **179,** 286–299 (2012).
14. Werner, B. T. & Kocurek, G. Bed-from dynamics: Does the tail wag the dog? *Geology* **25,** 771–774 (1997).
15. Nishimori, H., Yamasaki, M. & Andersen, K. H. A simple model for the various pattern dynamics of dunes. *Int. J. Mod. Phys. B* **12,** 257–272 (1998).
16. Parteli, E. J. R., Durán, O., Tsoar, H., Schwämmle, V. & Herrmann, H. J. Dune formation under bimodal winds. *Proc. Natl Acad. Sci. USA* **106,** 22085–22089 (2009).
17. Hesp, P., Hyde, R., Hesp, V. & Zhengyu, Q. Longitudinal dunes can move sideways. *Earth Surf. Process. Land.* **14,** 447–451 (1989).
18. Rubin, D. M., Tsoar, H. & Blumberg, D. G. A second look at western Sinai seif dunes and their lateral migration. *Geomorphology* **93,** 335–342 (2008).
19. Bristow, C. S., Bailey, S. D. & Lancaster, N. The sedimentary structure of linear sand dunes. *Nature* **406,** 56–59 (2000).
20. Lancaster, N. Assessing dune-forming winds on planetary surfaces—application of the gross bedform normal concept. *LPI Contributions* **1552,** 39–40 (2010).
21. Elbelrhiti, H., Claudin, P. & Andreotti, B. Field evidence for surface-wave-induced instability of sand dunes. *Nature* **437,** 720–723 (2005).
22. Narteau, C., Zhang, D., Rozier, O. & Claudin, P. Setting the length and timescales of a cellular automaton dune model from the analysis of superimposed bed forms. *J. Geophys. Res.* **114,** F03006 (2009).
23. Ha, S., Dong, G. & Wang, G. Morphodynamic study of reticulate dunes at southeastern fringe of the Tengger Desert. *Sci. China* **42,** 207–215 (1999).
24. Zhang, K., Qu, J. & An, Z. Characteristics of wind-blown sand and near-surface wind regime in the Tengger Desert, China. *Aeolian Res.* **6,** 83–88 (2012).
25. Kennedy, J. The mechanics of dunes and antidunes in erodible bed channels. *J. Fluid Mech.* **16,** 521–544 (1963).
26. Jackson, P. S. & Hunt, J. C. R. Turbulent wind flow over a low hill. *Q. J. R. Meteorol. Soc.* **101,** 929–955 (1975).
27. Rubin, D. M. & Hunter, R. E. Why deposits of longitudinal dunes are rarely recognized in the geologic record. *Sedimentology* **32,** 147–157 (1985).
28. Rubin, D. M. Lateral migration of linear dunes in the Strzelecki Desert, Australia. *Earth Surf. Process. Landf.* **15,** 1–14 (1990).
29. Dong, Z., Wang, T. & Wang, X. Geomorphology of the megadunes in the Badain Jaran Desert. *Geomorphology* **60,** 191–203 (2004).
30. Wilcock, P. Streamlab: Full-scale experiments in river science. *AGU (Fall Meeting)* Eos Trans. 90, abstr. No. EP31D-01 (2009).

Acknowledgements

We are grateful to O. Rozier, D. Rubin, M. Holschneider and S. Rodriguez for helpful discussions. We acknowledge financial support from the National Natural Science Foundation of China (no 41130533 and 41271021), the UnivEarthS LabEx program of Sorbonne Paris Cité (ANR-10-LABX-0023 and ANR-11-IDEX-0005-02), the French National Research Agency (ANR-09-RISK-004/GESTRANS and ANR-12-BS05-001-03/EXO-DUNES), the French Chinese International laboratory SALADYN and the city of Paris. Images of Fig. 1 are courtesy of Google Earth.

Author contributions

L.P. and Z.D. designed the experimental study. Z.Z. carried out the field measurements. L.P. carried out all statistical data analysis. C.N., Z.D. and S.C.d.P. designed the research and wrote the manuscript. All authors discussed the results.

Additional information

Supplementary information is available in the online version of the paper. Reprints and permissions information is available online at www.nature.com/reprints. Correspondence and requests for materials should be addressed to L.P. or C.N.

Competing financial interests

The authors declare no competing financial interests.